IEEE Access
Multidisciplinary ⋮ Rapid Review ⋮ Open Access Journal

Received June 30, 2021, accepted July 19, 2021, date of publication July 26, 2021, date of current version August 2, 2021.

Digital Object Identifier 10.1109/ACCESS.2021.3099535

Soft Frequency Reuse With Allocation of Resource Plans Based on Machine Learning in the Networks With Flying Base Stations

MD. SAKIR HOSSAIN[1,2], (Member, IEEE), AND ZDENEK BECVAR[1], (Senior Member, IEEE)
[1]Faculty of Electrical Engineering, Czech Technical University in Prague, 166 27 Prague, Czech Republic
[2]Department of Computer Science, American International University-Bangladesh, Khilkhet, Dhaka 1229, Bangladesh

Corresponding author: Zdenek Becvar (zdenek.becvar@fel.cvut.cz)

This work was supported by the Czech Science Foundation (GACR) under Grant P102-18-27023S.

ABSTRACT Flying base stations (FlyBSs) enable ubiquitous communications in the next generation mobile networks with a flexible topology. However, a deployment of the FlyBSs intensifies interference, which can result in a degradation in the throughput of cell-edge users. In this paper, we introduce a flexible soft frequency reuse (F-SFR) that enables a self-organization of a common SFR in the networks with an unpredictable and dynamic topology with the FlyBSs. We propose a graph theory-based algorithm for an allocation of resource plans, which is understood as a bandwidth allocation and a transmission power setting in the context of SFR. Furthermore, we introduce a low-complexity implementation of the proposed resource allocation using deep neural network (DNN) to significantly reduce the computation complexity. We show that the proposed F-SFR increases the throughput of cell-edge users by 16% to 26% and, at the same time, improves the satisfaction of the cell-edge users by up to 25% compared to the state-of-the-art solutions. We also demonstrate that the proposed scheme ensures a higher fairness in the throughput among the users with respect to the state-of-the-art solutions. The implementation via DNN also outperforms all state-of-the-art solutions despite its very low complexity.

INDEX TERMS Flying base station, interference, soft frequency reuse, deep neural networks, throughput, UAV, user satisfaction, fairness.

I. INTRODUCTION

The current mobile networks are typically based on a fixed infrastructure. Such architecture limits performance in scenarios, where the communication is supposed to be established in a highly time-space varying manner. To increase flexibility of the mobile networks, base stations can be mounted on unmanned aerial vehicles (UAVs) [1]. Such base stations are denoted as flying base stations (FlyBSs). The FlyBSs bring benefits in an emergency scenario and/or in situations with a significant short-to-mid-term increase in data traffic in a small area, for example, during sport events or concerts. To make the networks with the FlyBSs practically feasible, still, many challenges should be solved including [2], [3]: placement of the FlyBSs, resource allocations, energy efficiency, trajectory optimization for prolonging FlyBS operational time, user association, or interference management.

The associate editor coordinating the review of this manuscript and approving it for publication was Miguel López-Benítez.

The positions of the FlyBSs change over time depending on the user density and communication requirements. The FlyBSs' movement results in a strong variation of interference in time and space. This makes the interference management in the network with FlyBSs even more challenging than in the conventional mobile networks. Unfortunately, the research work in the interference management for the networks with the FlyBS is rather limited. The existing interference suppression or mitigation techniques exploit different network parameters, such as antenna type, power control, FlyBS positioning, and coordinated multi-point (CoMP). The directional antenna and antenna arrays are used in [4] and [5], respectively. However, the use of multiple antennas is practically not feasible for the FlyBSs due to a relatively small size of the FlyBSs. Interference management techniques based on CoMP are proposed in [6], [7]. However, the CoMP requires a significant number of signaling exchange among the FlyBSs and synchronization among different FlyBSs for CoMP operation. Some techniques optimize the positions of the FlyBSs

This work is licensed under a Creative Commons Attribution 4.0 License. For more information, see https://creativecommons.org/licenses/by/4.0/

[8]–[10], and transmission power [11]. Such techniques have, however, a high computational overhead due to the iterative nature of the optimization algorithms.

The above-mentioned works suffer from a high computation complexity and/or from a significant signaling load imposed by an exchange of control information. This limits practical applications of the FlyBSs, as the FlyBSs are of a limited processing capability and a limited energy. Moreover, the FlyBSs are designed to change positions, as the served users move. Hence, the positions of the FlyBSs are hard to predict and do not follow any predictable pattern. Therefore, the distance among FlyBSs can change over time significantly and, consequently, impairs the throughput. The most critical situation is for the cell-edge users, who get affected the most due to interference. A soft frequency reuse is a suitable solution to handle interference to the cell-edge users. Moreover, the SFR is of a low complexity and is easy to implement comparing to the above-mentioned solutions, as demonstrated in, e.g., [12]–[19]. Various strategies of implementing the SFR in the common mobile networks are presented in [12]–[20]. However, all these papers assume the locations of the base stations are apriori known and do not change over time. Although all above-mentioned solutions can improve the throughput of the cell-edge users in the conventional mobile network with a fixed and apriori known topology, a direct application of these works to the scenarios with FlyBS is not possible, because of a dynamic, irregular, and unpredictable topology of such networks.

In the common mobile networks, the SFR is implemented so that each cell is allocated with a specific resource plan, i.e., with a particular combination of the transmission power and the bandwidth assigned to the users in different levels of the cell. The resource plans are allocated to the cells in such a way that the cell with a particular resource plan is surrounded by a group of the cells with different resource plans. However, the positions of the FlyBSs are not known apriori, as the FlyBSs move according to the users behavior. This makes the locations of the FlyBSs unpredictable and such a 'fluid' nature of the topology of the networks with the FlyBSs does not allow a simple adoption of the common SFR. To the best of our knowledge, no effort has been made so far to adopt the SFR to the network with the FlyBSs to reduce interference.

To enable the use of the SFR in the networks with the FlyBSs, we propose a novel flexible SFR (F-SFR) allocating the resource plans dynamically according to the users' density, the number of FlyBSs, and the coverage area of individual FlyBSs. Unlike the solutions proposed in the related works, the proposed F-SFR supports an arbitrary number of SFR levels and the core idea enables an implementation via deep neural networks to lower the complexity of our solution.

The contributions of the paper are summarized as follows:

- We propose a novel graph theory-based algorithm that distributes the resource plans among the FlyBSs such that the interference experienced by the cell-edge users is reduced. The interference reduction is achieved via a smart allocation of the resource plans so that each FlyBS is allocated with the resource plan that maximizes the distance to another FlyBS with the same resource plan.
- While the number of resource plans in the existing approaches for SFR is confined to three, we propose a novel dynamic solution with the bandwidth allocation suitable for an arbitrary number of the resource plans. We show that a higher number of the resource plans results in an improvement in the throughput of the cell edge users.
- Since the networks with the FlyBSs are highly constrained by the computational capability and the energy, we devise the DNN-based resource plan allocation. The DNN is trained offline with the inputs represented only by the locations of the deployed FlyBSs. Then, the trained DNN predicts the resource plan for each FlyBS with a negligible complexity. The prediction is done simply by processing the actual positions of the FlyBSs via the trained DNN.

Note that this paper is an extension of our prior work [21], where an initial idea of the SFR in the networks with the FlyBSs is outlined. The overall motivation of this paper has evolved from the initial concept of a dynamic allocation of the resource plans presented in [21] to the low-complexity solution of the dynamic resource plan allocation. To this end, we propose a new low-complexity solution that assigns resource plans to the FlyBSs for the SFR via deep neural network. The new scheme is denoted as DNN F-SFR. Furthermore, while the number of resource plans in the existing approaches (including our prior work [21]) for the SFR is limited to three, in this paper, we propose a dynamic solution with the bandwidth allocation scheme suitable for an arbitrary number of the resource plans.

The rest of the paper is organized as follows. We provide an overview of related work in the next section. The system model is presented in Section III. The details of the proposed graph-theory-based F-SFR, its extension towards an arbitrary number of resource plans, and a low-complexity implementation via the DNN, are described in Section IV. Then, we evaluate the performance of the proposed F-SFR via simulations and compare it with the state of art schemes in Section V. Finally, the paper is concluded in Section VI.

II. RELATED WORK

Although a significant progress has been achieved in the research related to the FlyBS deployment [22]–[27], the only limited amount of works target the interference management among FlyBSs. In [28], interference management commonly adopted for small cells is applied to the networks with FlyBSs. The algorithm is based on non-cooperative game theory and allocates the channels among different FlyBSs so that co-channel interference is minimized. This results in a reduced interference among the FlyBSs. However, the overall

performance drops notably when the FlyBSs become overloaded. Furthermore, to eliminate the co-channel interference among the users of different FlyBSs, directional antennas at the FlyBSs are used in [4]. Another approach, presented in [5], jointly optimizes the user association, downlink transmission power, and three-dimensional placement of the FlyBSs to reduce interference. The gain in throughput is achieved via large antenna arrays. However, due to a limited processing capability and energy at the FlyBSs, the use of the large antenna arrays or directional antennas is not practical, as it incurs a heavy computational burden.

A deployment of multiple FlyBSs with awareness of interference is proposed in [29]. The FlyBSs are deployed at the center of non-overlapping circles. Hence, the distance of each FlyBS with respect to the center FlyBS is optimized to reduce interference. This approach is similar to the 7-cell clustering in the conventional mobile networks. Although such clustering reduces interference, the users' satisfaction rate is degraded as well, since the users' locations and their requirements are not considered. In [6], a user association and an interference mitigation are addressed. The authors propose an algorithm based on the CoMP to suppress the interference. The CoMP for the interference suppression in the networks with the FlyBSs is also proposed in [7]. The users are divided into a number of groups and the users in the same group are allocated with the same time and frequency in a particular epoch. Contrary, the users in different groups are allocated with orthogonal time and frequency. Nevertheless, this resource allocation results in a lower frequency reuse. Moreover, the CoMP requires an exchange of a notable amount of signalling among the FlyBSs to coordinate the communication in a perfectly synchronized manner. Nevertheless, the perfect synchronization might be impossible to guarantee in practical applications. In [8], [9], the FlyBS is deployed between a pair of a transmitter and a receiver to manage interference from a macro base station. The FlyBS acts as a relay and the interference is suppressed by an adjustment of the FlyBS's position. Since the FlyBS acts as the relay for a single link, interference among the FlyBSs is not considered.

A joint trajectory and power control-based interference management is proposed in [30], where relaying via multiple FlyBSs is assumed and neighboring macro base stations, small cells, and jammers are considered as a sources of interference. The trajectories of the FlyBSs are optimized by the spectral graph theory and, then, the transmission power of the FlyBSs is optimized. Nevertheless, the proposed optimization is highly complex in terms of computation, thereby, not efficient for the energy-constrained networks with the FlyBSs. In [11], the throughput maximization for a simple network with two FlyBSs and one user attached to each FlyBS is solved via a determination of the FlyBSs' locations and the allocation of the transmission power for each user. However, the proposed solution is very complex if more than two FlyBSs and multiple users are considered. In [10], interference among the FlyBSs is mitigated via the altitude optimization, as the altitude has a direct impact on the interference experienced by the users. However, only one user per FlyBS is considered and an extension to the scenario with multiple FlyBSs and multiple users is not straightforward.

In [31], [32], Q-learning is exploited for the transmission power control to improve the throughput by reducing interference in the heterogeneous networks. A similar approach is adopted for the association of the users in [33], [34]. Machine learning, by means of support vector machine, is adopted also in [35], [36] for the power control in cognitive radio networks. The power control is addressed via a deep neural networks in [37]. However, all these works are designed for the networks with a fixed infrastructure and a flexibility of the FlyBSs is not reflected. Machine learning for the networks with FlyBSs is considered, for example, in [38], where the authors optimize the FlyBSs' trajectory with interference awareness. However, the proposed algorithm incurs a significant computation overhead, which makes the interference mitigation complicated.

The cell-edge users get affected the most significantly due to the interference. A SFR is a less complex solution to handle interference to the cell-edge users. In [12], the cells are divided into more than two circular regions, denoted as levels, with the center of each region (level) located at the cell center. Such approach is known as multi-level SFR (ML-SFR) and allows an efficient mitigation of interference. In [13], the impact of a cell sectorization for the ML-SFR is investigated. An efficiency of the ML-SFR in heterogeneous networks (HetNets) is investigated in [14] and the SFR is found to be a savior for the cell-edge users [12]–[14]. A feasibility of the SFR in the scenario with microcells is analyzed in [15]. The authors in [15] develop the SFR for the HetNets combining the macrocells and the microcells. While the macrocell coordinates the allocation of the resource plans among the microcells, the microcells select the resource plan according to the reference signal received quality from the other microcells within the macrocell. However, without the macrocell being present, the algorithm is not applicable and implementable. In addition, similar to all existing SFR-based schemes, only three resource plans are considered in [15] and an extension towards a higher number of the resource plans is not straightforward due to the nature of the proposed solution. A three-level ML-SFR for the heterogeneous networks is then proposed in [16] to balance the communication load between the macrocells and the microcells. In [17], [18], the SFR is combined with CoMP to further improve throughput in the cell-edge area. An analysis of massive multiple-input multiple-output (MIMO) with SFR is carried out in [19]. In [20], an extreme learning machine predicts three parameters of SFR: i) the number of users in the cell-edge area, ii) the amount of bandwidth required for the cell-edge area, and iii) the power ratio of the cell-edge and cell-center area. The model proposed in [20] suffers from a high computational complexity due to the use of genetic algorithm. Furthermore, the allocation of resource plan is static.

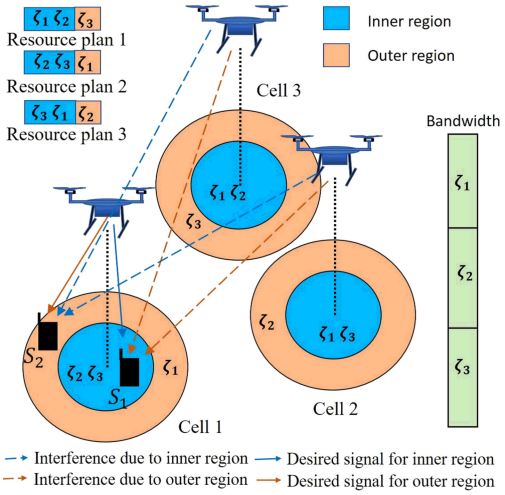

FIGURE 1. Interference scenario of SFR. (a) Interference of 2-level SFR (b) Bandwidth splitting.

III. SYSTEM MODEL

In this section, we outline the system model. Note that to keep a continuity, we follow a similar system model as in our prior work [21], where the SFR in the networks is outlined. In a common SFR, the cell is divided into L circular regions, denoted as levels. The center of each circular region (level) is located at the cell center [12]–[14]. For practical purposes, the number of levels L is an even number. If the cell is divided into more than two levels, the corresponding system is called multi-level SFR (e.g., 4-level SFR if $L = 4$). One SFR is created by two concrete levels in each cell, as shown in Fig. 1 for the 2-level SFR with the FlyBSs. The l^{th} level of the cell forms one SFR together with the $(L-l+1)^{th}$ level of the same cell. Note that $l \leq L$ and $l \in \mathbf{Z}^{+}$. For example, if $L = 8$ and $l = 2$, the second level forms the SFR with the seventh level of the cell. As two levels create one SFR, the number of the SFRs is equal to $\frac{L}{2}$ [13], [14].

The area covered by the l^{th} level is denoted as an inner region if $l \leq \frac{L}{2}$; otherwise, it is denoted as an outer region. The amount of the bandwidth allocated to the outer region of the SFR is a half of that allocated to the inner region to optimize the network throughput, see, e.g., [12]. In general, three cells form a cluster to ensure that the outer-regions of the cells in the cluster have a distinct bandwidth, as the whole bandwidth is divided into $L + \frac{L}{2}$ sub-bands. For example, in Fig. 1, the whole bandwidth is divided into three sub-bands: $\boldsymbol{\zeta} = \{(\zeta_1, \zeta_2, \zeta_3\}$ for $L = 2$, i.e., for 2-level SFR. The bandwidth allocated to the outer region of the cell is used in the inner regions of the cells in the same cluster [12]. The sub-bands are allocated to different levels of the cell with different transmission powers. The transmission power for communication with the users in the inner regions is lower than the transmission power for the users in the outer region [12]. A particular combination of the sub-band allocation to the different levels of the SFR and the corresponding transmission power setting is denoted as a resource plan. The total number of resource plans used in the network is denoted as N. To allocate a distinct bandwidth in the outer region of the cells in the cluster, $L + L/2$ sub-bands are created to form three resource plans as shown in Fig. 1 (upper-left corner of the figure) for $L = 2$.

The resource plan allocation starts from an arbitrary cell. In this cell, the sub-band allocation to different levels is also selected randomly out of all available options. In our example, the sub-bands ζ_1 and ζ_2 are allocated to the inner region with a low transmission power and ζ_3 is allocated to the outer region with a high transmission power in the cell 3. This combination of the sub-bands and the transmission powers is labeled as the resource plan 1. Similarly, the resource plan 2, with the sub-bands ζ_3 and ζ_2 for the inner region and ζ_1 for the outer region, is allocated to the cell 1. The last resource plan 3 is allocated to the cell 2. The power allocated to the sub-bands of the l^{th} level is defined, according to [14], as:

$$P_i = \begin{cases} \alpha_l \gamma_l P & \text{for } 1 \leq l \leq \frac{L}{2} \\ \alpha_{L-l+1} P & \text{for } \frac{L}{2} < l \leq L \end{cases} \tag{1}$$

where α_l is the ratio of the transmission power allocated to the outer level of the l^{th} SFR to the maximum transmission power P, and γ_l is the ratio of the transmission power allocated for the inner region to the power for the outer region of the l^{th} SFR level.

We assume that the users are uniformly distributed in a given area covered by M FlyBSs. Without loss of generality, the heights of the users are considered negligible. The FlyBSs can be deployed using any existing technique, such as those proposed in [23], [27], which maximize the network throughput. For the sake of simplicity of explanations, we adopt the deployment of the FlyBSs proposed in [23]. This deployment is based on k-means++ unsupervised machine learning algorithm [39]. As an optimization of the users' association is not our objective, we simply adopt a common association of the users to the FlyBSs so that the user is attached to the FlyBS from which it receives the strongest signal.

The throughput of the n^{th} user located in the l^{th} level of the m^{th} FlyBS is defined as:

$$\Gamma^{l}_{m,n} = B^{l}_{m,n} log_2 \left(1 + \frac{P_l g_{m,n}}{I_{=m} + I_{\neq m} + B^{l}_{m,n}\sigma^2}\right) \tag{2}$$

where $B^{l}_{m,n}$ is the bandwidth allocated to the n^{th} user located in the l^{th} level of the m^{th} FlyBS, $I_{=m} = \sum_{q \in \Omega_{=m}} P_l g_{q,n}$ is the interference from the FlyBSs in which the same resource plan as in the m^{th} FlyBS is used, $I_{\neq m} = \sum_{q' \in \Omega_{\neq m}} P_{L-l+1} g_{q',n}$ is the interference from the FlyBSs using different resource plans than the m^{th} FlyBS, $g_{m,n}$ is the channel gain between the m^{th} FlyBS and the n^{th} user of the m^{th} FlyBS, $\Omega_{=m}$ is the set of FlyBSs in which the same resource plan as in the m^{th} FlyBS is used, $\Omega_{\neq m}$ is the set of FlyBSs in which different resource plans compared to the m^{th} FlyBS are exploited, $g_{q,n}$ is the channel gain between the n^{th} user and the q^{th} FlyBS with $q \in \Omega_{=m}$, $g_{q',n}$ denotes the channel gain between the n^{th} user and

the q'^{th} FlyBS with $q' \in \Omega_{\neq m}$, P_{L-l+1} is the transmission power of the FlyBS for its $(L-l+1)^{th}$ level, and σ^2 is the noise power spectral density. Note that we use bold letter to present sets and matrices throughout the paper. A list of the symbols used in this paper is given in Table 1.

TABLE 1. List of symbols.

Symbols	Meaning
L	No. of levels in a cell
ζ	No. of sub-bands
P_l	Transmission power for the level l
α_l	Ratio of the transmission power allocated to the outer level of the l^{th} SFR to the maximum transmission power P
γ_l	Ratio of the transmission power allocated for the inner region to the power for the outer region of the l^{th} SFR level
M	No. of FlyBSs
$B^l_{m,n}$	Bandwidth allocated to the n^{th} user located in the l^{th} level of the m^{th} FlyBS
$g_{m,n}$	Channel gain between the m^{th} FlyBS and the n^{th} user of the m^{th} FlyBS
σ^2	Noise power spectral density
$\mathbf{U}^A$	Set of FlyBSs which are already allocated with resource plans
$\mathbf{U}^N$	Set of FlyBSs which are not yet allocated with any resource plans
R	Number of resource plans
$\mathbf{R}$	Set of resource plans
r_r	r^{th} resource plan
$D_{T,m}$	Distance between the *target* FlyBS and m^{th} FlyBS
$\mathbf{C}$	Set of resource plans already allocated to FlyBSs
c_m	The resource plan allocated to the m^{th} FlyBS
S	The *Start* FlyBS
δ_r	Distance of the *closest* FlyBS with the r^{th} resource plan from the *target* FlyBS
$\mathbf{D}^*$	Set of distances of all FlyBSs with the r^{th} resource plan from the *target* FlyBS
$\Gamma^l_{m,n}$	Throughput of the n^{th} user under m^{th} FlyBS's l^{th} level
Γ_{min}	The minimum throughput requirement of a user

IV. PROPOSED F-SFR FOR NETWORKS WITH FlyBSs

In this section, we first outline the targeted problem and we motivate the approach adopted to solve this problem. Then, we address the challenges caused due to the variable radius of the FlyBS's cell and the resource plans allocation among the FlyBSs in a dynamic and flexible manner. To this end, we describe also an assignment of the users to individual levels of the cells. Afterwards, we introduce the proposed algorithm for a flexible allocation of the resource plans. Furthermore, we present an extension of the proposed SFR towards the bandwidth allocation for an arbitrary number of resource plans. We also introduce a low-complexity scheme for allocation of the resource plans based on DNN.

A. OUTLINE OF THE PROBLEM AND MOTIVATION FOR THE ADOPTED APPROACH

The objective is to improve the throughput of cell-edge user via the proposed SFR tailored for the flexible networks with the FlyBSs while the maximum transmission power, P, is not increased and the fairness among the users is not impaired. This objective is addressed via the proposed F-SFR described in the next subsections. To use the SFR in the networks with FlyBSs, any two FlyBSs with the same resource plans should be positioned as far as possible from each other. One way to facilitate this is to apply a SFR-aware deployment of the FlyBSs in which the objective is to maximize the minimum distance between any two FlyBSs with the same resource plan. This optimization problem can be solved using any nature-inspired optimization algorithm, such as genetic algorithm, particle swarm optimization, etc. Such solution converges to the deployment of the FlyBSs at the edges of the served area to suppress interference. However, at the same time, it also decreases the network throughput, as the received signal from the serving FlyBSs is also of a low quality due to a relatively large distance between the user and the FlyBSs. Another approach to solve our problem is a multi-objective optimization to jointly maximize the minimum distance between any two FlyBSs having the same resource plan and the network throughput. In this case, the gain in the throughput of cell-edge users is achieved by sacrificing the network throughput and vice-versa. As our objective is to suppress interference, we focus on the resource plan allocation for already deployed FlyBSs. This allows us to design an algorithm independent of the FlyBSs' deployment in order to make our solution universal. Thus, the FlyBSs can be deployed to maximize the network throughput via any of the existing positioning algorithm.

The flowchart of the proposed F-SFR is shown in Fig. 2. First, the FlyBSs are deployed using k-means++ algorithm. We adopt k-means++, as it is simple, but efficient and commonly adopted solution in many related works. As the k-means++ only serves for the deployment of the FlyBSs, it is always performed at the beginning of the algorithm. Then, the users are associated to the FlyBSs and to a specific level of SFR. After this step, the resource plans are allocated for all FlyBSs either via the proposed graph-theory-based or DNN-based approach. Finally, power and bandwidth are allocated to each user depending on the resource plan allocated to the FlyBS. In the next subsections, we first describe the association of the users (to the FlyBSs and to the SFR levels) and, then, we describe the allocation of the resource plans to the individual SFR levels of each FlyBS. We also present an extension of the proposed F-SFR towards an allocation of an arbitrary number of the resource plans and to a low-complexity solution based on the DNN.

B. ASSOCIATION OF THE USERS

The user association in SFR involves two steps: association of the users to different FlyBSs and, then, association of

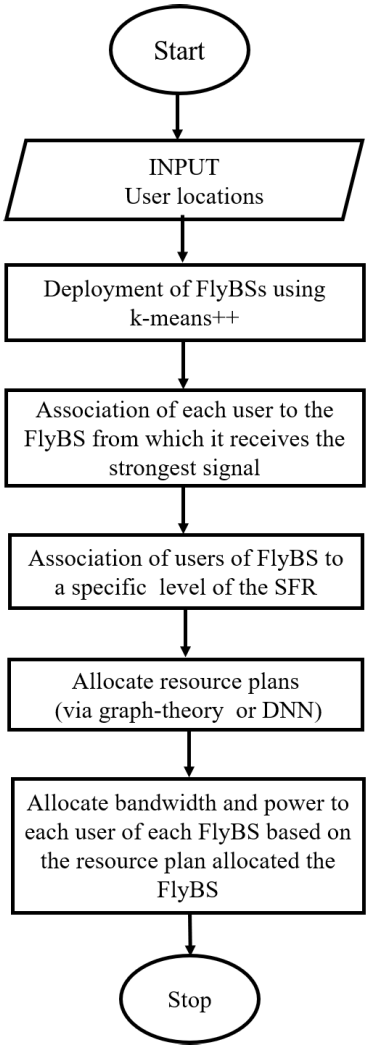

FIGURE 2. Flowchart of the proposed resource plan allocation in networks with FlyBSs.

the users of each FlyBS to different levels of the FlyBS. As the principle of our proposed resource plan allocation for the F-SFR is independent of the users' association to the FlyBSs, we adopt the technique proposed in [40], where the user is attached to the FlyBS from which it receives the strongest signal compared to that from all other FlyBSs. Once the users are matched to the FlyBSs, the users should be also associated to the individual levels of SFR. The simple solutions developed solely for the 2-level SFR, such as the one in [15], are unfortunately not directly applicable to our targeted ML-SFR. Thus, we propose the following approach enhancing the convectional association developed for the 2-level SFR towards ML-SFR.

First, we arrange the users associated to each FlyBS in the ascending order depending on the strength of the received signal from the respective FlyBSs. In the common SFR, the outer region is allocated with a half of the bandwidth of its corresponding inner region [12]. Also, in the conventional SFR, the radius of each level is determined in such a way that the outer region contains a half of the users associated to the inner region of the SFR [15]. For this reason, we divide the sorted users into $L + L/2$ groups. Compared to the users in the second and other groups, the users in the first group receive stronger signals. The inner and outer regions of the SFR are allocated with two and one groups of the users, respectively. Among $L + L/2$ groups of the users, the users of the first two groups (i.e., those receiving the highest and second highest levels of signal from the FlyBS) are associated with the level 1, while the users in the last group (i.e., those receiving the lowest level of signal from the FlyBS) are associated with the last level of the FlyBS. The remaining groups of the users are, then, associated with the rest of the levels sequentially considering whether the levels belong to the inner-region or the outer-region. For example, for 4-level SFR, the first two groups of the users are associated with the first level, the next two groups are associated to the second level. Then, the fifth and sixth groups of the users are associated with the third and fourth levels, respectively.

C. PROPOSED ALLOCATION OF THE RESOURCE PLANS

Once the users are associated to the SFR levels of each FlyBS, the bandwidth for each SFR level should be allocated. The allocation of bandwidth for different levels of the FlyBSs should be done with respect to the bandwidth allocation for the neighboring FlyBSs in the cluster, because the bandwidth allocated in the outer region of any SFR of one FlyBS cannot be used in any outer region of any SFR of the neighboring FlyBSs. This bandwidth allocation results in a reduced interference experienced by the cell-edge users and in an increase in their throughput. However, the resource plans should be allocated among the FlyBSs so that two FlyBSs having the same resource plans are as far as possible from each other. To solve this challenge, we propose and describe a novel approach for the allocation of the resource plans among the FlyBSs based on the graph theory.

In the network with the FlyBSs, we can consider each FlyBS as a vertex of a graph. Then, connecting the vertices to each other, we create the complete graph, where the edge between a pair of the vertices represents the distance between the vertices. The complete graph represents the locations of different FlyBSs and the distances between the FlyBSs. An example of such graph consisting of five vertices (i.e., FlyBSs) is shown in Fig. 3. After representing the networks

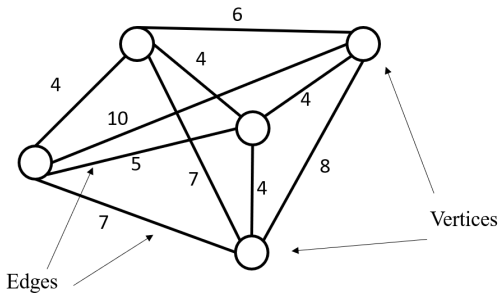

FIGURE 3. Representation of the networks with FlyBSs as graph.

with the FlyBSs as the complete graph, we introduce the concept of the graph coloring problem (the vertex coloring in particular). However, instead of using the vertex adjacency constraint (i.e., two adjacent vertices must have different colors), we modify the constraint so that *the vertices should be colored such that the distance between any two vertices of the same color is maximized*. To color the graph, we consider a fixed number of colors, where the color represents one resource plan. In other words, we determine the color of each vertex (i.e., assign the resource plans to the FlyBSs) out of the given the number of colors (i.e., the number of resource plans). In this way, the problem of allocating the resource plan to the FlyBSs is transformed into the graph coloring problem. Note that the complete graph of M vertices consists of $\frac{M(M-1)}{2}$ edges.

First, we give a brief high-level overview of the proposed algorithm before explaining it in detail. The algorithm starts with a random selection of one FlyBS, which is denoted as the *start FlyBS*. This FlyBS is allocated with any of the available resource plans. Out of the rest of the FlyBSs, the FlyBS located closest to the *start FlyBS* is selected for the allocation of another resource plan in the next iteration. The FlyBS selected for the next iteration is denoted as the *target FlyBS*. All FlyBSs that have some resource plans already allocated are grouped according to their plans so that the FlyBSs with the same plan are in the same group. In each group, the FlyBS that is the closest to the *target FlyBS* is determined and we denote it as the *closest FlyBS*. Note that the number of the *closest FlyBSs* is equal to the number of groups of the FlyBSs with the same resource plan. Then, among the *closest FlyBSs*, the one that is the farthest from the *target FlyBS* is chosen (we label it as the *farthest FlyBS*). This chosen FlyBS (the *farthest FlyBS*) determines the resource plan for the *target FlyBS* so that the *target FlyBS* is allocated with the same resource plan as the *farthest FlyBS*. In the next step, a new *target FlyBS* is selected out of the FlyBSs, which are not allocated with any resource plan yet and the process is repeated until all FlyBSs get one resource plan.

Now, let's describe the proposed solution in more details. First, we define few variables to describe the proposed solutions in Algorithm 1. The FlyBSs are divided into two groups: i) the FlyBSs, which *are already allocated* with the resource plans (these are included in the set $\boldsymbol{U}^A$), and ii) the FlyBSs, which are *not yet allocated* with any resource plan (included in the set $\mathbf{U}^N$). Initially, $\mathbf{U}^A$ is an empty set while $\mathbf{U}^N$ contains all FlyBSs. The set $\mathbf{R} = \{r_1,\ r_2,\ \ldots, r_R\}$ contains all available resource plans r_r and R is the number of available resource plans. The set $\mathbf{C}$ maps the assigned resource plans to the FlyBSs so that the m^{th} element of $\mathbf{C}$ contains the resource plan assigned to the FlyBS indicated in the m^{th} element of $\mathbf{U}^A$. Note that $\mathbf{C}$ is initially an empty set.

In the first step of the resource plan allocation, the *start FlyBS* S is randomly selected from $\mathbf{U}^N$ (line 2 in Algorithm 1). The *start FlyBS* S is allocated with any random resource plan (r_r) and this fact is reflected by putting r_r to the set $\mathbf{C}$ (line 3). The FlyBS is then included to the $\mathbf{U}^A$ and excluded from $\mathbf{U}^N$ (line 3). Then, the distances $d_{S,m}$ of all FlyBSs in $\mathbf{U}^N$ from the *start FlyBS* are calculated (line 5) and the *closest FlyBS* is selected (line 6) as the *target FlyBS* T for the next iteration.

Algorithm 1: Resource Plan Allocation

```
1  U^A ← ∅, U^N ← 1 : M, R ← [r_1, r_2, r_R], C ← ∅
2  Select the start FlyBS, S, randomly from U^N
3  C ← C ∪ r_1, U^A ← U^A ∪ S, U^N = U^N \ S
4  while |U^N| > 0 do
5      Determine d_{S,m} ∀m ∈ U^N
6      T ← argmin_{m∈U^N} d_{S,m}
7      for r ← 1 to |R| do
8          D* ← ∅
9          for m ∈ U^A do
10             if r == c_m then
11                 Determine d_{T,m}
12                 D* ← D* ∪ d_{T,m}
13             end
14         end
15         δ_r ← min(D*)
16     end
17     r* ← argmax_{r∈R} δ_r
18     C ← C ∪ r*, U^A ← U^A ∪ T, U^N ← U^N \ T
19 end
```

The distance of each FlyBS to the *start FlyBS* can be calculated either from known coordinates of all FlyBSs or from the level of signal received from other FlyBSs using a cellular localization technique [41]. Note that coordinates of the FlyBSs should be known for a common operation and flight control of the FlyBSs, hence, such assumption is perfectly realistic in any real-world applications of the FlyBSs. As the interference mitigation is critical especially in the scenarios, where the FlyBSs can interfere with each other (i.e., there are no buildings or obstacles among them), we can assume that even the second approach for the determination of the distance based on the received signal levels is feasible. The reason is that we can assume that there are no obstacles/buildings among the FlyBSs as the obstacles/buildings would suppress mutual interference and any inter-cell interference mitigation technique would not be needed. Hence, the mutual received signal levels among the FlyBSs can properly reflect the distances among the FlyBSs in a realistic scenario.

For each resource plan (line 7), the distances $d_{T,m}$ of the *target FlyBS* T to all FlyBSs $c_m \in \mathbf{C}$ already allocated with the given resource plan $r \in \mathbf{R}$, (lines 9-10), are calculated (line 11) and stored in $\mathbf{D}^*$. In line 9, $|\mathbf{C}|$ denotes the cardinality of the set $\mathbf{C}$. Then, the distance δ_r of the *closest FlyBS* with the r^{th} resource plan from the *target FlyBS* is determined (line 15). Note that if there is no FlyBS with any of the r^{th} resource plan up to this iteration, that is, $\mathbf{D}^*$ is empty, the distance is set to infinity. However, if three source plans

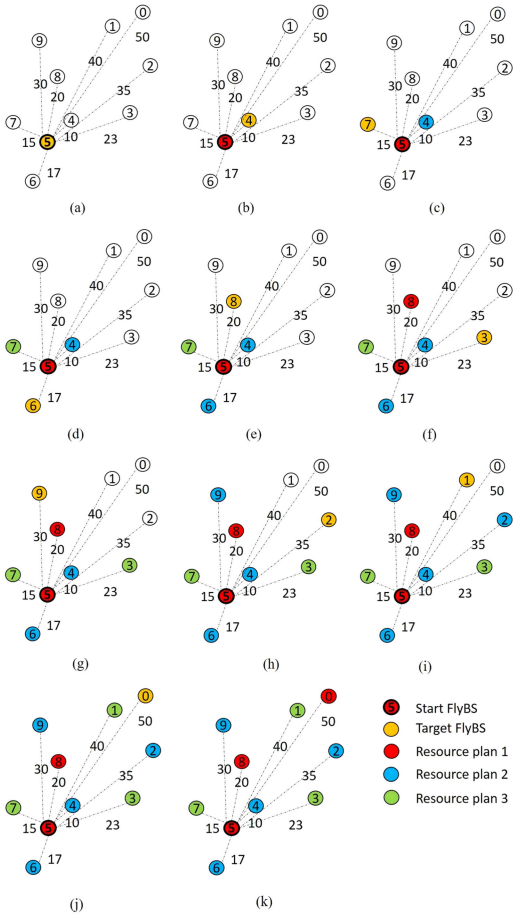

FIGURE 4. Example of the allocation of resource plans to FlyBSs; FlyBSs are depicted with circles and the number in the circle indicates ID of the FlyBS, each color corresponds to a specific resource plan, the distances among the FlyBSs are indicated by the numbers between the FlyBSs.

would be available, three closest FlyBSs with the distances δ_r are found (line 15) so that one FlyBS uses each of the resource plans. Next, among the *closest FlyBSs* (in our example three FlyBSs), the resource plan r^* of the *farthest FlyBS* is allocated to the *target FlyBS* (lines 17-18). Note that if two or more FlyBSs are in the same distance, a random FlyBS out of these is selected. Finally, the FlyBS is inserted to $\mathbf{U}^A$ and excluded from $\mathbf{U}^N$ (line 18). After this allocation, the new iteration starts by selecting the new FlyBS from $\mathbf{U}^N$ as the *target FlyBS* and the above process is repeated.

In order to clarify the proposed algorithm explained above, we assume a network of 10 FlyBSs (see Fig. 4(a)). Let us assume that the FlyBS 5 is chosen arbitrarily as the *start FlyBS*. An arbitrary resource plan is allocated to the FlyBS. In the figure, the resource plan 1, shown with red color in Fig. 4, is randomly selected for the FlyBS. Next, we select the FlyBS, which is the closest to the FlyBS 5 but is not assigned with any resource plan yet. The selected *closest FlyBS*, which is FlyBS 4 in this case, is allocated with the resource plan next. The FlyBS 4 is labeled as *target FlyBS* in this iteration. To know which resource plan to allocate to the *target FlyBS*, we compute distance of the *target FlyBS* from all FlyBSs, which are already allocated with the resource plans. The FlyBS 5 is the closest FlyBS to the *target FlyBS* and is assigned with the resource plan 1. Thus, we can allocate any resource plan except the resource plan 1 to the FlyBS 4. In this case, we randomly pick the resource plan 2, from the resource plans 2 and 3, which is presented as blue color in Fig. 4(c). Afterwards, we select the new *target FlyBS* to allocate the resource plan. As before, the *target FlyBS* is the *start FlyBS's* closest FlyBS among all the FlyBSs, which has no resource plan yet. As shown in Fig. 4(d), the FlyBS 7 is the new *target FlyBS*. The FlyBS 5 and 4 are allocated with the resource plans 1 and 2, respectively. Thus, the new *target FlyBS*, FlyBS 7, is allocated with the resource plan 3 (green color), i.e., with the only resource plan not allocated so far. Now, each resource plan is allocated exactly once.

In the next iteration, the FlyBS 6 is the closest FlyBS from the *start FlyBS* among the FlyBSs, which are yet not allocated with the resource plan. Hence, we select the FlyBS 6 as the new *target FlyBS*. Since we have at least one FlyBS per resource plan, we group the FlyBSs, which are already allocated with the resource plans based on their resource plans. This gives us three groups: group1 (FlyBS 5 with plan 1); group 2 (FlyBS 4 with plan 2); and group 3 (FlyBS 7 with plan 3). We have only one FlyBS per group. Thus, the FlyBS of each group is the closest FlyBS to the *target FlyBS* 6 from the respective group. Thus, the FlyBS 4 is the farthest FlyBS out of the three FlyBS (one from each group). The *target FlyBS* 6 is allocated with the resource plan of the farthest FlyBS 4. Thus, the resource plan 2 is allocated to the FlyBS 6. Afterwards, we select a new *target FlyBS* for the next iteration.

Now, to show the process for a general case with more FlyBSs already associated with the resource plans, let's skip to Fig. 4(h). The FlyBSs 3, 4, 5, 6, 7, 8, and 9 are already allocated with the resource plans. Still the FlyBSs 0, 1, and 2 are not yet allocated with any resource plan. Out of the three FlyBSs with no resource plan, the FlyBS 2 is the closest to the *start FlyBS*. Thus, we denote the FlyBS 2 as the new *target FlyBS*. To know the resource plan, which should be allocated to the *target FlyBS*, let us divide the FlyBSs already allocated with the resource plans into three groups based on their resource plans. We get three groups: group 1 (FlyBSs 8 and 5 with plan 1), group 2 (FlyBSs 6, 4 and 9 with plan 2) and group 3 (FlyBSs 3 and 7 with plan 3). Next, we select the closest FlyBS to the *target FlyBS* 6 from each group. For the group 1, out of the FlyBS 8 and 5, the FlyBS 8 is the closest one to the FlyBS 2. Thus, we select the FlyBS 8 from the group 1. Similarly, we find the FlyBSs 4 and 3 from the groups 2 and 3, respectively. Out of the FlyBSs 2, 3 and 8, the FlyBS 4 is the farthest from the *target FlyBS* 2. Thus, the resource plan of the FlyBS 4, i.e., the plan 2, is allocated to the FlyBS 2 as shown in Fig. 4 (i). This process repeats until we allocate the resource plan to every FlyBS. The final resource plan allocation to all FlyBSs is shown in Fig. 4(k). We see that the FlyBSs 0, 5 and 8 are allocated with the

resource plan 1 (red), the FlyBSs 2, 4, 6, and 9 are allocated with the plan 2 (blue), and the plan 3 (green) is allocated to the FlyBSs 1, 3, and 7.

D. BANDWIDTH ALLOCATION FOR ARBITRARY NUMBER OF RESOURCE PLANS

The conventional SFR takes into account a pre-defined three cells set up (i.e., $N = 3$) to form a cluster to allocate the bandwidth among the different levels. The reason behind choosing only three cells for the allocation of the bandwidth in the conventional SFR schemes is to ensure that the cell with a particular resource plan is surrounded by the cells with different resource plans. However, there exists no such fixed pattern of the resource plans allocation among the cells in the network with FlyBSs. Under this scenario, we have an extra degree of freedom and we can discard such constraint. Hence, we discuss a way how to use more than three FlyBSs (i.e., $N \geq 3$) to form a soft cluster. We introduce the term soft cluster to indicate that the cluster of FlyBSs with the relative positions of the FlyBSs is not fixed and changes over time depending on the user distribution at a specific time instant (e.g., due to users' movement).

The major motivation for the higher value of N is that we can increase the mutual distance between any two FlyBSs with the same resource plan and, thus, the interference is suppressed. This situation is illustrated in Fig. 5. While Fig. 5(a) shows the resource plan allocation for $N = 3$, the same deployment of the FlyBSs for $N = 6$ is shown in Fig. 5(b). Comparing both examples for $N = 3$ and $N = 6$, we see that there is a significant increase in the distance between the FlyBSs with the same resource plans due to a higher number of the resource plans. The increased distance reduces interference among the FlyBSs and, consequently, improves the spectral efficiency in the cell-edge area.

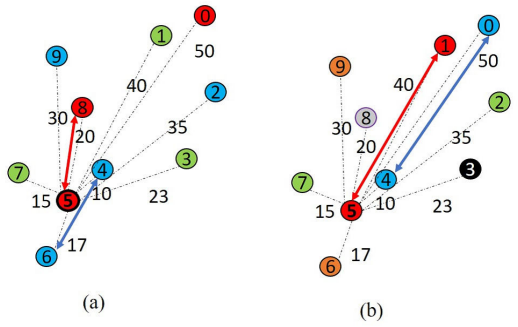

FIGURE 5. Example of the effect of the using higher number of resource plans: (a) three resource plans (b) six resource plans.

Since each FlyBS uses a distinct sub-band in its cell-edge area with respect to the other FlyBSs in the soft cluster, the required number of the resource plans is N and the required number of the sub-bands is $\frac{L}{2}N$. Figure 4 shows an example of the sub-bands allocation among different SFR levels of each FlyBS of the soft cluster for $N = 6$. The number of sub-bands allocated to all levels except the outer-most level of each FlyBS is $N - 1$. Thus, the higher number of resource plans results in the allocation of a wider band to the inner region comparing to the outer region. Since the users are divided among different levels based on their channel quality, the number of users considered to be the cell-edge users decreases. However, the reduced number of the users experiences comparatively higher throughput due to the increased number of the resource plans. The increased number of the resource plans allows to use the same resource plan farther from each other to reduce interference and, consequently, to increase the throughput of the cell-edge users.

E. LOW-COMPLEXITY IMPLEMENTATION OF PROPOSED F-SFR VIA DNN

The performance of the network with the FlyBSs is highly constrained by a limited processing capability of the FlyBSs and by a limited energy available for both flying and communication. The computation demanding algorithms for the resource plans allocation result in a higher energy consumption. In addition, complex solutions escalate the network response time in a fast-changing environment. However, the proposed resource plan allocation algorithm is of the polynomial time complexity $O(M^2N)$. To reduce the complexity, we develop the resource plan allocation algorithm based on machine learning that can save a large part of the computation overhead. To this end, the inputs and outputs of the graph-theory based solution can be used to train any machine learning model, which can classify patterns. The model should discover the pattern in the input data and finds an association between the pattern and the output. This association approximates the behavior of the algorithm (i.e., how the algorithm reacts to the pattern of its input data). Once the model learns the behavior of the algorithm, it can mimic that behavior and the learned model becomes an abstraction of the algorithm. Since the model just mimics the algorithm, it does not follow the procedure the algorithm itself. For this reason, the computational overhead of the model-based solution is significantly lower than that of the algorithm itself. Approximating the graph theory-based algorithm, we propose a deep neural network-based F-SFR (DNN F-SFR). We select the DNN for the algorithm approximation, because the DNN is proven to be suitable for functions approximation, as shown, e.g., in [42]. The DNN is known to handle very complex problems due to its capability of extracting patterns even from a large dataset. Unlike the classification algorithms, such as K-nearest neighbor (KNN), which requires a lot of computation in predicting the class of an instance of the dataset, the DNN requires only a very little computation. This property makes the DNN very suitable for the networks with the FlyBSs, as the FlyBSs are limited by the energy available in the battery. Thus, we use the DNN instead of other classification algorithms to reduce complexity of the F-SFR. Another reason for which the DNN is used to approximate our graph theory-based resource plan allocation algorithm is that, unlike any other traditional classification algorithms, it does not require an explicit feature selection and it can

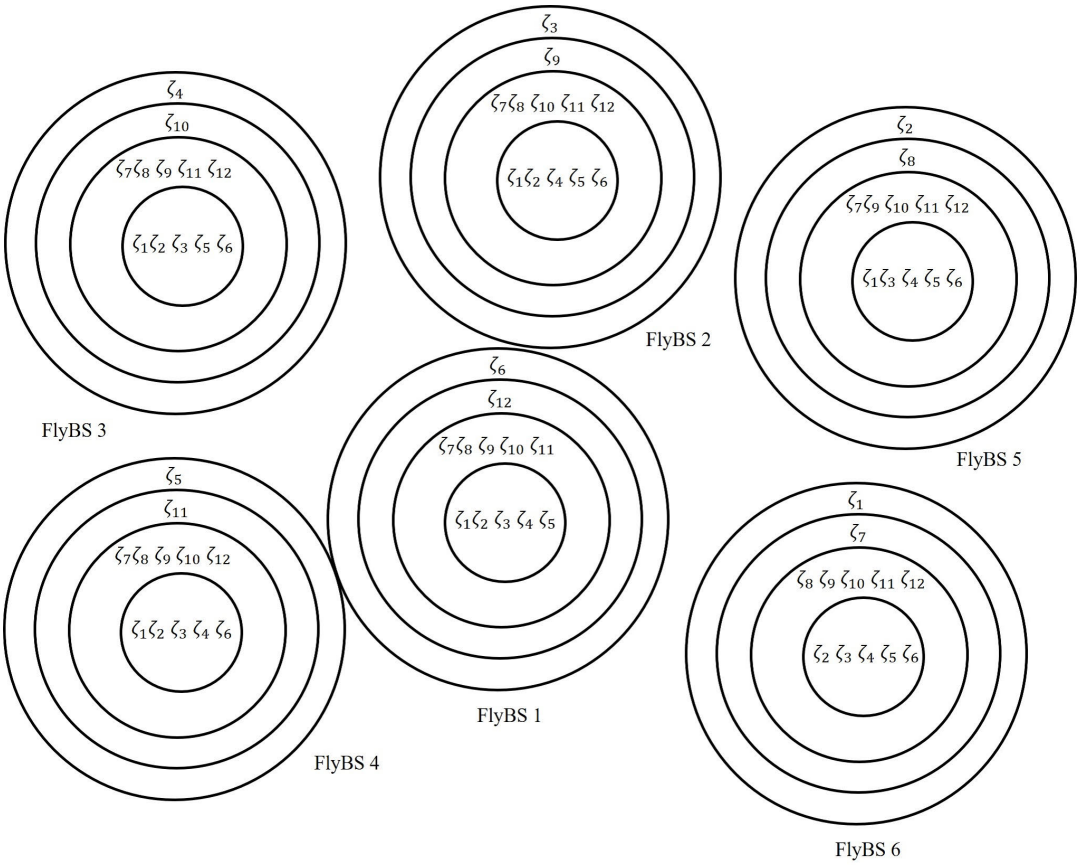

FIGURE 6. Allocation of sub-bands, ζ, to the SFR levels and FlyBSs in a soft cluster for $N = 6$.

select the most important features by itself exploiting its multiple layers. This makes the DNN suitable in terms of computational overhead [43].

The implementation of DNN involves the DNN training and the prediction of the resource plan allocation. The DNN is trained offline and, then, it promptly predicts the resource plans of the individual FlyBSs online during a real operation of the FlyBSs. The training is done with an artificially created dataset, as any real dataset is not unavailable. Nevertheless, the real datasets are usually not necessary to validate basic ideas and concepts and simulation-based data sets are commonly considered in literature [42], [44]–[46]. The DNN consists of three hidden layers and one input and one output layer as shown in Fig. 7. The inputs to the network are represented by the locations of FlyBSs determined by the k-means++, as explained in Section III. We consider two-dimensional deployment of the FlyBSs with a fixed altitude. Thus, the input layer is composed of $2M$ neurons for the network with M FlyBSs, each neuron representing either X or Y coordinate of one FlyBSs. The number of neurons in the output layer is equal to the number of available resource plans N. In the first, second, and third hidden layers, 19, 13, and 14 neurons are included, respectively. The number of hidden layers and the number of neurons in the hidden layers are determined experimentally and lead to a good performance while the size of the DNN is still acceptable.

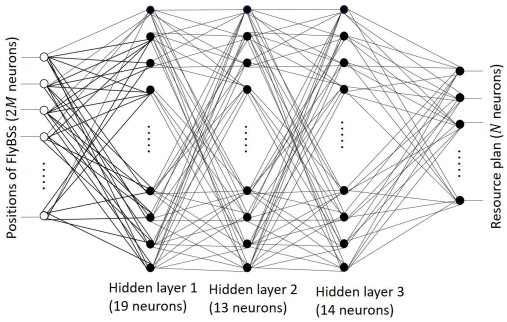

FIGURE 7. Illustration of DNN structure for prediction of resource plan allocation for FlyBSs.

The step-by-step operation of the DNN based solution is presented in Fig. 8 and Fig. 9. Fig. 8 shows the steps of the dataset creation and offline training of the DNN. The training of the DNN requires the dataset. The dataset creation starts from the generation of the random user locations with the uniform distribution. The FlyBSs are positioned in the area applying k-means++ clustering algorithm. The positions are, then, inserted to the graph theory-based resource plan allocation algorithm (summarized in Fig. 2), which allocates the resource plans to all FlyBSs in the network. Each instance of the dataset contains the positions of all FlyBSs and the

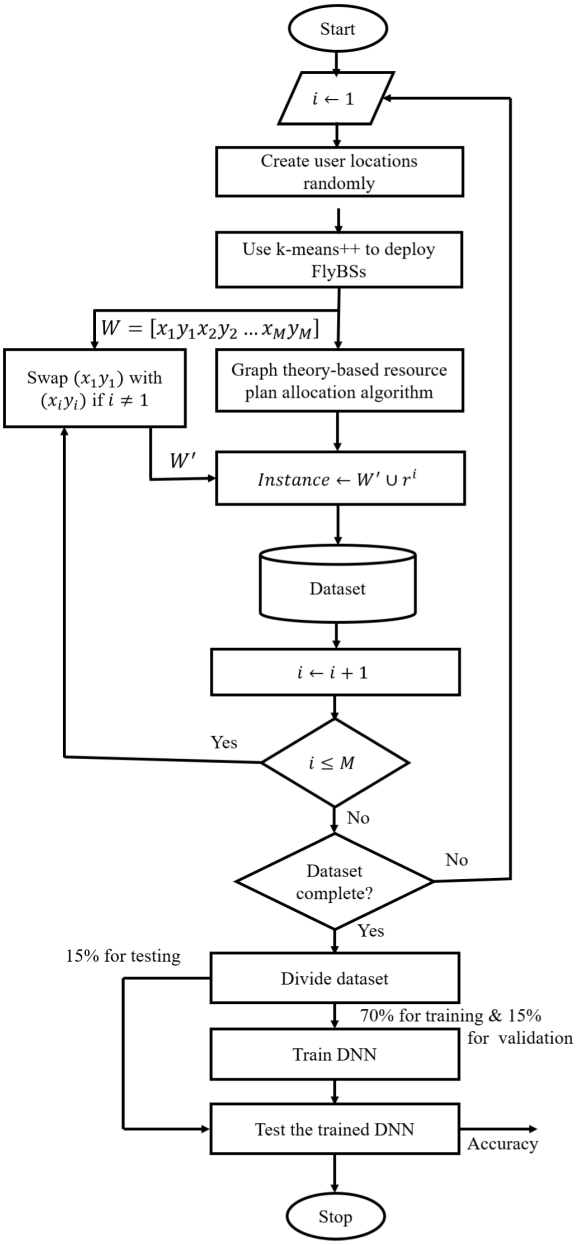

FIGURE 8. Flowchart of dataset creation and training of the DNN for the proposed DNN F-SFR.

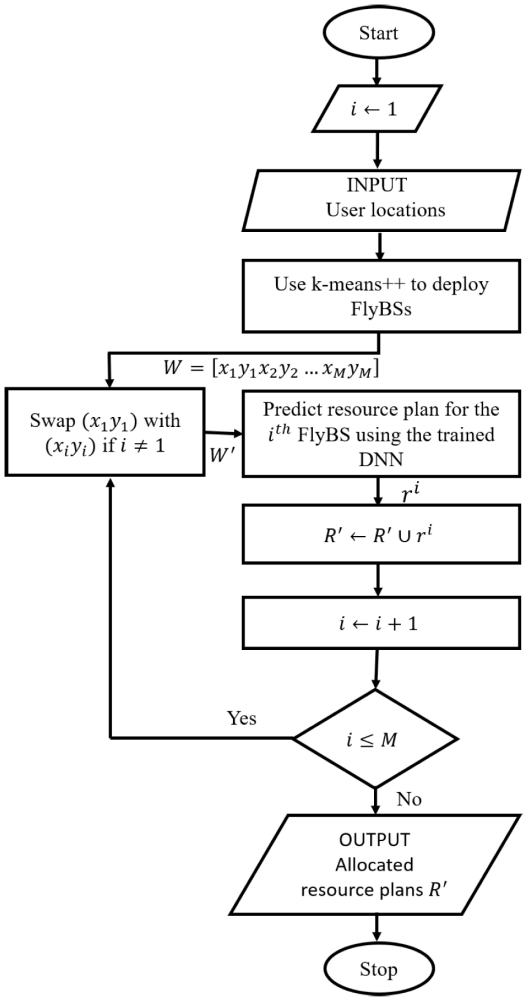

FIGURE 9. Flowchart of the online testing of the DNN F-SFR.

resource plan number (i.e., the label or class of the instance) for the FlyBS, whose actual position is represented by the first two elements of the input vector $\mathbf{W}$. To get the instance representing the resource plan of the i^{th} FlyBS, the locations of the first and the i^{th} FlyBSs are swapped (by swapping 1^{st} and 2^{st} elements with the $(2i-1)^{th}$ and $2i^{th}$ of $\mathbf{W}$) and, then, the i^{th} element of the output of the resource plan allocation algorithm is appended at the end of the position vector $\mathbf{W}$. There are $M-1$ swapping operations performed to generate M instances of the dataset if there are M FlyBSs in the network. Thereafter, the new vector of the FlyBSs' positions is generated based on the new positions of the users. This process continues until the required number of instances is generated. After generating the dataset, the 70%, 15% and 15% of the whole dataset are exploited for the training, validation, and testing, respectively. While the training and validation datasets are used for the offline DNN training, the test dataset is exploited for evaluation of the proposed resource plans allocation performance to verify how correctly the DNN can mimic the behavior of the graph theory-based resource plan allocation algorithm.

Fig. 9 gives the pictorial representation of the DNN's exploitation. The trained DNN is used for online allocation of the resource plans. The DNN-based resource plan allocation starts with inserting the positions of the users to the k-means++ clustering algorithm, which determines the positions of the FlyBSs. Then, the trained DNN allocates one resource plan to each FlyBS in each iteration. To know the resource plan of the i^{th} FlyBS, we again swap the $(2i-1)^{th}$ and $2i^{th}$ elements (represents the position of the i^{th} FlyBS) with the 1^{st} and 2^{nd} elements (represents the position of the 1^{st} FlyBS) of the input FlyBS position vector $\mathbf{W}$. Then, we apply this modified position vector $\mathbf{W}'$ to the input layer of the DNN. For M FlyBSs, there are M iterations, and each

iteration assigns the resource plan to one FlyBS (represented by the vector $\mathbf{R}'$).

F. DESIGN FEATURES AND POTENTIAL CONSTRAINTS

In this subsection, following basic features of the proposed approach and potential constraints and extensions are described. The proposed solutions follow a centralized approach. One of the FlyBSs acts as the 'leader', which coordinates the network deployment. First, the FlyBSs are deployed using the k-means++ clustering algorithm. Then, either the F-SFR or the DNN F-SFR is run to allocate the resource plans among the FlyBSs. However, the DNN F-SFR can also be implemented in distributed manner. The distributed approach requires each FlyBS to transmit its position and share it with others so that each FlyBS gets the positions of all FlyBSs. Knowing the positions, each FlyBS runs the trained DNN to know its own resource plans. Although the resource plans can be allocated in the distributed manner using the proposed DNN F-SFR, the deployment of the FlyBSs is still centralized if the conventional k-means++ or any other algorithm are used for this purpose. In future works, the determination of the FlyBSs' positions can enhance our work to optimize performance via positioning done jointly with the interference mitigation. Another important design feature is the capability of the proposed solutions to adopt any number of resource plans. In case of the moving users, the deployment of the FlyBSs and allocation of the resource plans among the FlyBSs should be done periodically. At the end of each period, the number of resource plans can be decided in our proposal depending on the throughput requirement of the cell-edge area, and the resource plans are allocated dynamically. This offers an extra degree of freedom with respect to existing works to optimize also the network performance depending on the serving environment.

Of course, the practical implementation of our solution implies additional challenges to be considered and addressed. For example, the distributed solution requires signaling among FlyBSs to let each other know positions of all FlyBSs. This signaling consumes communication resources and, in real applications, a small portion of the available resources should be reserved for this purpose. However, this problem is also present for HetNet SFR and other existing approaches. In this paper, the parameter setting of the DNN is done experimentally. However, the considered parameters may not be optimum as any optimization algorithm is not used in this paper. Thus, a possible extension can optimize the DNN parameters over time to further improve performance. However, such optimization adds a computational burden on the FlyBSs, which are of a limited processing capability. Hence, a trade-off between performance and computation should be taken into account.

V. PERFORMANCE EVALUATION

In this section, we first define simulation scenarios, models and parameters. Then, the performance metrics are defined and simulation results are presented along with their discussion.

A. SIMULATION SCENARIO AND MODELS

A suburban area with a size of 1 km $\times$ 1 km is considered. In this area, 400 users are randomly distributed and also up to 24 FlyBSs are deployed according to k-means++ algorithm [39]. Although the proposed resource plan allocation algorithm can be applied to any FlyBS positioning systems, we consider k-means++ algorithm in this paper for its simplicity and good performance [47]. To model the communication channel, the path loss model of air-to-air channel is taken from [48] and the pathloss between the users and the FlyBSs corresponds to the model for the suburban environment as defined in [49]. The parameters related to the simulation environment are set up in line with [47]. The bandwidth is equally divided among the users located within a particular SFR level of the FlyBS. The simulation parameters are summarized in Table 2. The values of the parameters for the transmission power allocation (α and γ, see (1)) are determined experimentally and set to the values leading to a sufficiently high performance. An optimization of these values dynamically according to the environment is a complex problem and we leave it for future research. To eliminate a randomness in the models, we consider 5000 realizations of the deployment, each realization is with different locations of the users and, thus, also with different locations of the FlyBSs. As indicated above in Section IV-E, we design the DNN with three hidden layers, each with 19, 13, and 14 neurons, respectively. The DNN is trained offline with artificial data. To minimize the overfitting problem, we exploit a validation set of data with a size of 15% of the whole dataset (see [50] for more details about the overfitting problem and the validation set). The detailed parameters of the DNN setting and configuration are given in Table 3.

TABLE 2. Simulation parameters.

Parameters		Values
Simulation area		1 km $\times$ 1 km
No. of FlyBSs		3 to 24
No. of users		400
Carrier frequency		2 GHz
Bandwidth		20 MHz
Transmission power		30 dBm
FlyBS height		20 m [27]
No. of SFR levels		2, 4
Noise power		-174 dBm
α	2-level	1
	4-level	[1 0.7]
γ	2-level	0.5
	4-level	[0.3 0.71]

B. BENCHMARK ALGORITHMS AND PERFORMANCE METRICS

We consider two state-of-the-art algorithms as benchmarks to assess the performance of the proposed F-SFR and DNN F-SFR. To show the gain of SFR in the networks with the

TABLE 3. Parameters of deep neural network for allocation of resource plans.

Parameters	Values
Training function	Levenberg-Marquardt backpropagation
Maximum no. of epochs	500
Learning rate	0.01
Hidden layer activation function	Tangent sigmoid
Output layer activation function	Softmax
Dataset size	130,000 samples
Training dataset	70%
Validation dataset	15% [50]
Test dataset	15%
Cost function	Mean square error (MSE)

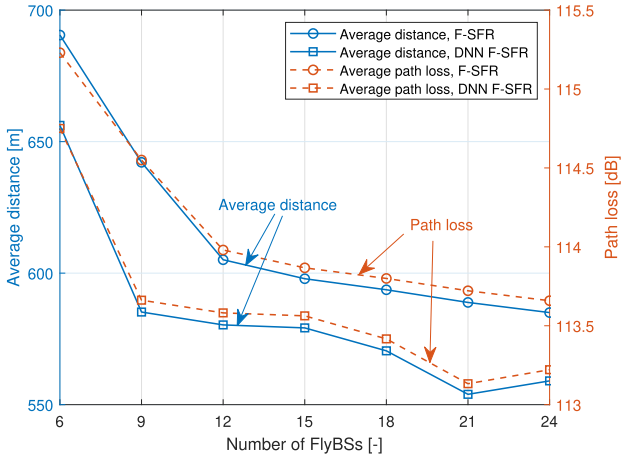

FIGURE 10. Accuracy of resource plan allocation for FlyBSs by DNN represented via average distance among the FlyBSs allocated with the same resource plan and projection of the average distance to path loss.

FlyBSs, we first consider a recent resource allocation scheme for the interference mitigation among FlyBSs proposed in [6], where each user is allocated with an equal transmission power and bandwidth. This approach is denoted as 'No SFR' in the figures. Then, also the SFR for heterogeneous networks, proposed in [15] and denoted as 'HetNet SFR', is investigated. The HetNet SFR is, up to our best knowledge, the only solution that considers the resource plan allocation to the randomly and irregularly deployed microcells. However, even this solution cannot be directly implemented to a general scenario with the FlyBSs. To make the HetNet SFR suitable for the network with FlyBSs, one of the FlyBSs is assumed to perform the role of the macrocell. For a fair comparison of the throughput, the user association scheme discussed in Section IV-B is used in all schemes.

The performance is evaluated in terms of the average throughput of cell-edge users, the ratio of satisfied cell-edge users for a minimum throughput requirement, and the fairness in throughput. The average throughput of cell-edge users is understood as the average throughput of the users associated to the outer-most level (e.g., the second and fourth levels for two and four-levels SFR, respectively). Note that, for the 'No SFR', the same set of users as for both F-SFR and HetNet SFR algorithms is defined as the cell-edge users for a fair comparison. The ratio of satisfied cell-edge users is understood as the ratio of the total number of users that experience the throughput equal to or higher than the minimum required throughput Γ_{min}. The fairness in throughput is investigated via a commonly accepted Jain's fairness index, see its definition, e.g., in [51].

C. ANALYSIS OF THE DNN ACCURACY

To investigate the quality of DNN learning, an accuracy is commonly considered. Our objective is to suppress mutual interference imposed by the FlyBSs via the allocation of the same resource plan to the FlyBSs that are far from each other. Hence, we define the accuracy of the DNN learning via the distance among the FlyBSs that cause interference to each other. More specifically, in Fig. 10, the accuracy is represented by the average distance among all FlyBSs that exploit the same resource plan. To provide an indication from a more practical perspective, we also interpret the accuracy via the average path loss among the FlyBSs with the same resource plan in Fig. 10. The figure demonstrates that the average distance among the FlyBSs with the same resource plan reached by the F-SFR (target of the DNN learning) and by the DNN-based F-SFR is very close to each other. The difference ranges from 4.9% and 4.4% for 6 and 24 FlyBSs, respectively. As the distances among the FlyBSs with the same resource plans are relatively high (hundreds of meters), such learning error is negligible. This is confirmed by a projection of the average distance to the path loss. Fig. 10 indicates that the difference in path loss between the F-SFR and the DNN F-SFR is below 0.9 dB (i.e., 0.7% error). Such error in the path loss of the interfering channels is negligible and we can conclude the learning is sufficiently accurate for the purposes of the interference suppression via SFR.

D. PERFORMANCE ANALYSIS OF THE PROPOSED RESOURCE ALLOCATION AND DISCUSSION OF RESULTS

First, we demonstrate the performance of the F-SFR in terms of the average throughput experienced by the cell-edge users in Fig. 11. This figure shows the throughput for both two- and four-level SFRs. We observe that the conventional interference mitigation technique, represented by the No SFR, is not efficient for an application in the networks with the FlyBSs and the No SFR is outperformed by all other SFR schemes, because interference in the cell-edge area is not sufficiently managed by the No SFR. Contrary, the proposed F-SFR significantly improves the throughput comparing to all other state-of-the-art schemes. The throughput improvement introduced by the F-SFR with respect to the No SFR and the HetNet-SFR is from 52% to 200% and from 16% to 26%, respectively. Fig. 11 further demonstrates an increasing gain in the throughput introduced by the proposed F-SFR over

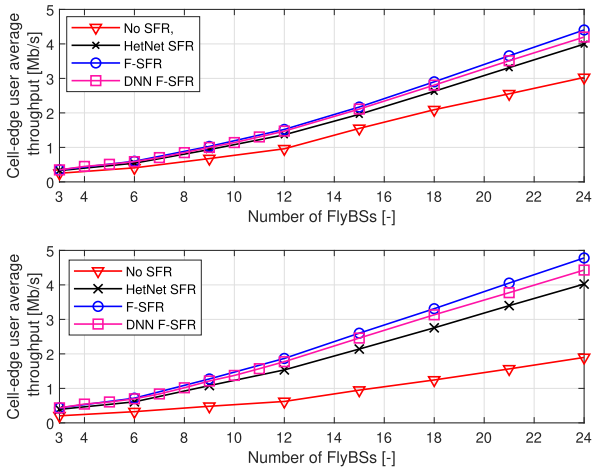

FIGURE 11. Average throughput of cell-edge users over different number of deployed FlyBSs for 2-layer SFR (top subplot) and 4-layer SFR (bottom subplot).

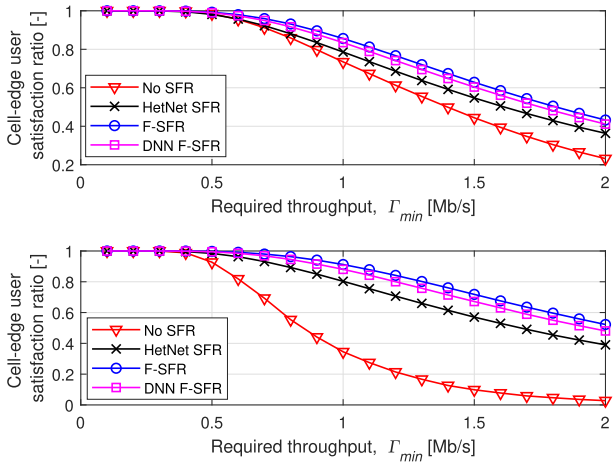

FIGURE 12. Ratio of satisfied cell-edge users, i.e., the cell-edge users that experience throughput equal to or above their minimum requirement Γ_{min} for scenario with 15 FlyBSs for 2-layer SFR (top subplot) and 4-layer SFR (bottom subplot).

the No SFR and the HetNet SFR if the number of FlyBSs increases. This observation is a result of the fact that, with a higher number of FlyBSs, the interference becomes more severe and the proposed F-SFR can handle it more efficiently, since it provides a high spatial separation of the same resource plans allocated to the FlyBSs. The figure also shows that the number of SFR levels influences the performance notably and the throughput rises with the number of levels. The 4-level F-SFR provides about 19% higher throughput than the 2-level F-SFR. The reason for the superior performance of the 4-level SFR over 2-level SFR is a lower interference resulting from the lower transmission power in the inner regions of the neighboring FlyBS. As the number of levels increases, the radii of the inner regions decrease, hence, a lower transmission power is set to the users located within the inner regions. Figure 11 also confirms that even the low-complexity DNN-based implementation of the F-SFR outperforms both No SFR and HetNet SFR. Of course, the lower complexity of the DNN F-SFR results into a minor degradation in the throughput of the cell-edge users with respect to the proposed F-SFR. However, this degradation is in order of few percent (about 5%) for both $L = 2$ and $L = 4$. The degradation is compensated by the much lower computational complexity of the DNN-SFR, making the DNN F-SFR a suitable resource plan allocation schemes for networks with the FlyBSs.

We investigate also the ratio of the cell-edge users for which, the minimum required throughput Γ_{min} is satisfied, see Fig. 12. The proposed F-SFR outperforms both the HetNet SFR and the No SFR for a whole investigated range of Γ_{min}. The maximum gain is reached for the throughput required by the users of 1.4 Mb/s. At this point, the proposed F-SFR leads to an increase in the ratio of the satisfied users by 484% (from 0.13 to 0.76) and by 25% (from 0.61 to 0.76) comparing to the No SFR and the HetNet SFR, respectively. It is worth to note that the increase in the number of SFR levels affects the satisfaction ratio in a different way for different algorithms. The satisfaction ratio increases for all schemes based on the SFR (i.e., DNN F-SFR, F-SFR, and HetNet SFR). The higher number of SRF levels significantly improves the performance of the proposed F-SFR, as the F-SFR can take an advantage of the higher number of the SFR levels via an efficient mitigation of interference. For the HetNet SFR, the ratio of the satisfied users improves only slightly with a higher number of levels L, as the distance between two neighboring FlyBSs with the same resource plan impacts more notably on the throughput of the cell-edge user than on the lower transmission power in the inner-most level of the neighboring FlyBS. The conventional interference mitigation, represented by the No SFR, leads even to a lower satisfaction for higher L. This is due to the fact that the average distance of the cell-edge users from the FlyBS in the 4-level SFR is larger than in the 2-level SFR. Hence, the cell-edge users experience strong interference and their throughput degrades. We also see that for $L = 4$, the DNN F-SFR offers up to 1634% (77% for $L = 2$) and 23% (13% for $L = 2$) higher ratio of the satisfied cell-edge users comparing to the No SFR and the HetNet SFR, respectively. The superiority of the proposed F-SFR is demonstrated by the fact that the percentage of the satisfied users obtained by the HetNet SFR with $L = 4$ is reached even by the DNN F-SFR with only $L = 2$.

While it is evident from the above discussion that the proposed F-SFR and DNN F-SFR improve the throughput and the user satisfaction, we investigate also the fairness in throughput of the users to demonstrate the fairness in throughput among the users located in the cell-center and cell-edge regions of the FlyBS.

Figure 13 shows that the proposed F-SFR reaches the highest fairness among all schemes overall numbers of FlyBSs and SFR levels. The highest fairness reached by the F-SFR is a results of the increased throughput of the cell-edge users. Consequently, a difference in the throughput among the users

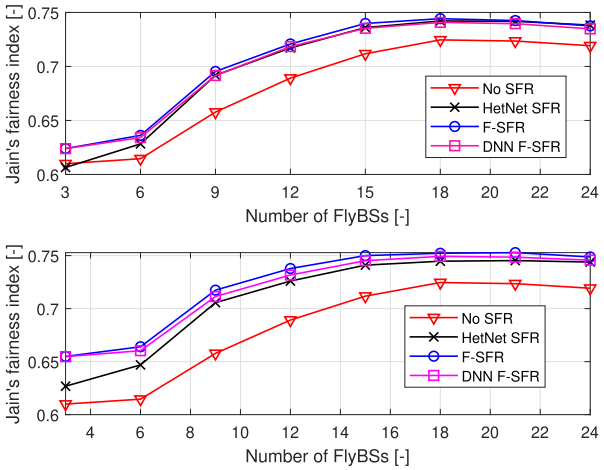

FIGURE 13. Fairness in throughput experienced by all users represented via Jain's Fairness Index for 2-layer SFR (top subplot) and 4-layer SFR (bottom subplot).

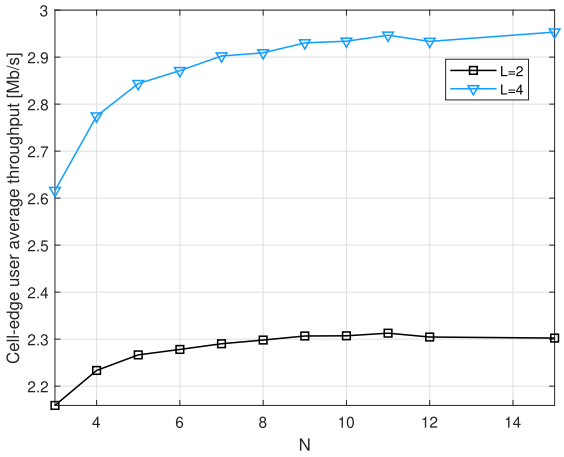

FIGURE 14. Impact of number of resource plans on the average throughput of cell-edge user achieved by the proposed F-SFR for 15 FlyBSs.

is reduced and the fairness is increased. In addition, a higher number of the SFR levels also increases the fairness. This is again a consequence of the increased throughput of the cell-edge users, as demonstrated in Fig. 11. For all schemes, the fairness increases with the number of FlyBSs up to a maximum reached around 18-20 FlyBSs. Then, the fairness saturates and starts slightly decreasing. The initial increase is due to the distance of the users to the FlyBS. For a lower number of the FlyBSs, the area covered by each FlyBS is larger comparing to the area covered if a higher number of the FlyBSs is deployed. Thus, there is a higher difference in the distances of the closest and farthest users from the serving FlyBS. Consequently, also a higher path loss difference among these two users is observed and this causes a more notable difference in the throughput (lower fairness). The increase in the number of FlyBS leads to a more balanced effect of the impact of an increasing interference among the FlyBSs and a decreasing path loss of the users to the serving FlyBS. Thus, the fairness rises with more deployed FlyBSs. However, any further increase in the number of FlyBSs makes the interference dominant over the pathloss and the throughput of the cell-edge and cell-center users becomes more different. For $L = 2$, the fairness of the low-complexity DNN F-SFR is almost the same as for the F-SFR and HetNet SFR. For $L = 4$, the fairness attained by the DNN F-SFR reaches slightly lower fairness (up to 1%) comparing to the proposed F-SRF and slightly higher fairness (up to 1%) compared to the HetNet SFR. Anyway, Fig. 13 confirms that the superior performance of both F-SFR as well as DNN F-SFR in terms of the cell-edge users' throughput is not at the cost of a lower fairness among the users.

The throughput of the cell-edge users can be further improved by increasing the number of the resource plans as shown in Fig. 14 for 15 FlyBSs. Note that the existing resource plan allocation algorithms, e.g., the one proposed in [15], are not directly applicable to the SFR with more than three resource plans. Thus, we do not depict the competitive algorithms in Fig. 14. The figure demonstrates that a higher number of the resource plans improves the throughput by up to roughly 15% and 7% for $L = 4$ and $L = 2$, respectively. This improvement is achieved for about 10 resource plans, then, there is no effect of the number of resource plans. This behavior can be explained as follows. Two FlyBSs with the same resource plan cause more interference to each other than the same two FlyBSs with the different resource plans. Then, for a lower number of the resource plans, any two FlyBSs with the same resource plans are relatively close to each other. However, if the number of resource plans increases, the distance among FlyBSs with the same resource plan increases as well and the interference is reduced. Once the distance among FlyBSs with the same resource plans is large enough and the interference among these FlyBSs with the same resource plan is negligible, any further increase in the number of resource plans (and thus in the distance among FlyBSs with the same resource plans) does not affect the throughput.

VI. CONCLUSION AND FUTURE WORK

In this paper, we have proposed a novel SFR scheme, named F-SFR, in order to dynamically and adeptly allocate resource plans among the FlyBSs in a coverage area depending on the current network topology. The objective of the resource plan allocation algorithm is to allocate the transmission power and bandwidth among different levels of the coverage area of each FlyBSs such that the distance between the FlyBSs allocated with the same resource is maximized. This maximization of the distance reduces interference. We show that with respect to the state-of-the-art SFR schemes, the proposed F-SFR attains a notable improvement in the cell-edge users' throughput. The improvement varies from 16% to 26% depending on the number of FlyBSs deployed in the service area. Furthermore, the proposed scheme achieves up to 25% improvement in the user satisfaction ratio in terms of the experienced throughput. In addition, the proposed F-SFR does not compromise fairness in throughput among the users. Furthermore, we have also proposed an extension enabling to

increase the number of resource plans resulting in additional up to 15% improvement in the throughput of the cell-edge users. Thus, we have designed also a very low-complexity implementation of the proposed F-SFR via DNN. This DNN-based F-SFR slightly reduces the gains of the F-SFR with respect to the state-of-the-art solutions, however, even the DNN-based F-SFR still significantly outperforms the state-of-the-art approaches.

As a future work, a joint FlyBSs deployment and resource plan allocation optimization should be investigated. Furthermore, the DNN-based solution with the real dataset should also be tested. Moreover, replacing the centralized approach with a distributed solution, where each FlyBS decides its position and resource plan is a future challenge.

REFERENCES

[1] F. Tariq, M. R. A. Khandaker, K.-K. Wong, M. A. Imran, M. Bennis, and M. Debbah, "A speculative study on 6G," *IEEE Wireless Commun.*, vol. 27, no. 4, pp. 118–125, Aug. 2020.

[2] A. A. Khuwaja, Y. Chen, N. Zhao, M.-S. Alouini, and P. Dobbins, "A survey of channel modeling for UAV communications," *IEEE Commun. Surveys Tuts.*, vol. 20, no. 4, pp. 2329–2345, Jul. 2018.

[3] M. Mozaffari, W. Saad, M. Bennis, Y.-H. Nam, and M. Debbah, "A tutorial on UAVs for wireless networks: Applications, challenges, and open problems," *IEEE Commun. Surveys Tuts.*, vol. 21, no. 3, pp. 2334–2360, 3rd Quart., 2019.

[4] E. Kalantari, I. Bor-Yaliniz, A. Yongacoglu, and H. Yanikomeroglu, "User association and bandwidth allocation for terrestrial and aerial base stations with backhaul considerations," in *Proc. IEEE PIMRC*, Oct. 2017, pp. 1–6.

[5] A. Fouda, A. S. Ibrahim, I. Guvenc, and M. Ghosh, "Interference management in UAV-assisted integrated access and backhaul cellular networks," *IEEE Access*, vol. 7, pp. 104553–104566, 2019.

[6] C. Wang, B. Hu, and S. Chen, "Joint user association and interference mitigation for drone-assisted heterogeneous wireless networking," *EURASIP J. Wireless Commun. Netw.*, vol. 2019, no. 1, p. 163, Dec. 2019.

[7] L. Liu, S. Zhang, and R. Zhang, "CoMP in the sky: UAV placement and movement optimization for multi-user communications," *IEEE Trans. Commun.*, vol. 67, no. 8, pp. 5645–5658, Aug. 2019.

[8] S. Hosseinalipour, A. Rahmati, and H. Dai, "Interference avoidance position planning in UAV-assisted wireless communication," in *Proc. IEEE Int. Conf. Commun. (ICC)*, May 2019, pp. 1–6.

[9] S. Hosseinalipour, A. Rahmati, and H. Dai, "Interference avoidance position planning in dual-hop and multi-hop UAV relay networks," *IEEE Trans. Wireless Commun.*, vol. 19, no. 11, pp. 7033–7048, Nov. 2020.

[10] Z. Zhang, L. Li, W. Liang, X. Li, A. Gao, W. Chen, and Z. Han, "Downlink interference management in dense drone small cells networks using mean-field game theory," in *Proc. 10th Int. Conf. Wireless Commun. Signal Process. (WCSP)*, Oct. 2018, pp. 1–6.

[11] X. Li and J. Xu, "Positioning optimization for sum-rate maximization in UAV-enabled interference channel," *IEEE Signal Process. Lett.*, vol. 26, no. 10, pp. 1466–1470, Oct. 2019.

[12] X. Yang, "A multilevel soft frequency reuse technique for wireless communication systems," *IEEE Commun. Lett.*, vol. 18, no. 11, pp. 1983–1986, Nov. 2014.

[13] M. S. Hossain, F. Tariq, and G. A. Safdar, "Enhancing cell-edge performance using multi-layer soft frequency reuse scheme," *Electron. Lett.*, vol. 51, no. 22, pp. 1826–1828, Oct. 2015.

[14] M. S. Hossain, F. Tariq, G. A. Safdar, N. H. Mahmood, and M. R. A. Khandaker, "Multi-layer soft frequency reuse scheme for 5G heterogeneous cellular networks," in *Proc. IEEE Globecom Workshops (GC Wkshps)*, Dec. 2017, pp. 1–6.

[15] G. Giambene, V. A. Le, T. Bourgeau, and H. Chaouchi, "Soft frequency reuse schemes for heterogeneous LTE systems," in *Proc. IEEE ICC*, Jun. 2015, pp. 3161–3166.

[16] G. Giambene, V. A. Le, T. Bourgeau, and H. Chaouchi, "Iterative multi-level soft frequency reuse with load balancing for heterogeneous LTE-A systems," *IEEE Trans. Wireless Commun.*, vol. 16, no. 2, pp. 924–938, Feb. 2017.

[17] J. Pastor-Perez, F. Riera-Palou, and G. Femenias, "Optimization of irregular CoMP-aided OFDMA networks with SFR: A multiobjective approach," in *Proc. IEEE VTC-Spring*, Jun. 2018, pp. 1–7.

[18] J. A. Pastor-Perez, F. Riera-Palou, and G. Femenias, "Analytical network-wide optimization of CoMP-aided MIMO-OFDMA irregular networks with frequency reuse: A multiobjective approach," *IEEE Trans. Commun.*, vol. 67, no. 3, pp. 2552–2568, Mar. 2019.

[19] Y. Li, R. Wang, and Z. Zhang, "Massive MIMO downlink goodput analysis with soft pilot or frequency reuse," *IEEE Wireless Commun. Lett.*, vol. 7, no. 3, pp. 448–451, Jun. 2018.

[20] M. F. Misran, M. I. Shapiai, R. A. Dziyauddin, and H. M. A. Jalil, "Parameter optimization for conventional soft frequency reuse in multi cell networks using extreme learning machine and genetic algorithm," *J. Telecommun., Electron. Comput. Eng.*, vol. 8, no. 11, pp. 23–28, 2016.

[21] M. Hossain and Z. Becvar, "Flexible soft frequency reuse for interference management in the networks with flying base stations," in *Proc. IEEE VTC-Spring*, May 2020, pp. 1–7.

[22] Z. Becvar, M. Vondra, P. Mach, J. Plachy, and D. Gesbert, "Performance of mobile networks with UAVs: Can flying base stations substitute ultra-dense small cells?" in *Proc. 23rd Eur. Wireless Conf.*, 2017, pp. 1–7.

[23] B. Galkin, J. Kibilda, and L. A. DaSilva, "Deployment of UAV-mounted access points according to spatial user locations in two-tier cellular networks," in *Proc. Wireless Days (WD)*, Mar. 2016, pp. 1–6.

[24] X. Liu, Y. Liu, and Y. Chen, "Reinforcement learning in multiple-UAV networks: Deployment and movement design," 2019, *arXiv:1904.05242*. [Online]. Available: http://arxiv.org/abs/1904.05242

[25] A. Fotouhi, M. Ding, and M. Hassan, "Flying drone base stations for macro hotspots," *IEEE Access*, vol. 6, pp. 19530–19539, 2018.

[26] W. Shi, J. Li, W. Xu, H. Zhou, N. Zhang, S. Zhang, and X. Shen, "Multiple drone-cell deployment analyses and optimization in drone assisted radio access networks," *IEEE Access*, vol. 6, pp. 12518–12529, 2018.

[27] J. Plachy, Z. Becvar, P. Mach, R. Marik, and M. Vondra, "Joint positioning of flying base stations and association of users: Evolutionary-based approach," *IEEE Access*, vol. 7, pp. 11454–11463, 2019.

[28] J. Chen, Q. Wu, Y. Xu, Y. Zhang, and Y. Yang, "Distributed demand-aware channel-slot selection for multi-UAV networks: A game-theoretic learning approach," *IEEE Access*, vol. 6, pp. 14799–14811, 2018.

[29] A. A. Khuwaja, G. Zheng, Y. Chen, and W. Feng, "Optimum deployment of multiple UAVs for coverage area maximization in the presence of co-channel interference," *IEEE Access*, vol. 7, pp. 85203–85212, 2019.

[30] A. Rahmati, S. Hosseinalipour, Y. Yapici, X. He, I. Guvenc, H. Dai, and A. Bhuyan, "Interference avoidance in UAV-assisted networks: Joint 3D trajectory design and power allocation," in *Proc. IEEE Global Commun. Conf. (GLOBECOM)*, Dec. 2019, pp. 1–6.

[31] M. Simsek, M. Bennis, and I. Guvenc, "Learning based frequency- and time-domain inter-cell interference coordination in HetNets," *IEEE Trans. Veh. Technol.*, vol. 64, no. 10, pp. 4589–4602, Oct. 2015.

[32] T. Sanguanpuak, S. Guruacharya, N. Rajatheva, M. Bennis, and M. Latva-Aho, "Multi-operator spectrum sharing for small cell networks: A matching game perspective," *IEEE Trans. Wireless Commun.*, vol. 16, no. 6, pp. 3761–3774, Jun. 2017.

[33] T. Kudo and T. Ohtsuki, "Cell range expansion using distributed Q-learning in heterogeneous networks," in *Proc. IEEE VTC Fall*, Sep. 2015, pp. 1–5.

[34] F. Pervez, M. Jaber, J. Qadir, S. Younis, and M. A. Imran, "Fuzzy Q-learning-based user-centric backhaul-aware user cell association scheme," *IEEE Access*, vol. 6, pp. 1840–1845, 1018.

[35] L. Xu and A. Nallanathan, "Energy-efficient chance-constrained resource allocation for multicast cognitive OFDM network," *IEEE J. Sel. Areas Commun.*, vol. 34, no. 5, pp. 1298–1306, May 2016.

[36] M. Lin, J. Ouyang, and W.-P. Zhu, "Joint beamforming and power control for device-to-device communications underlaying cellular networks," *IEEE J. Sel. Areas Commun.*, vol. 34, no. 1, pp. 138–150, Jan. 2016.

[37] M. Najla, D. Gesbert, Z. Becvar, and P. Mach, "Machine learning for power control in D2D communication based on cellular channel gains," in *Proc. IEEE Globecom Workshops (GC Wkshps)*, Dec. 2019, pp. 1–6.

[38] U. Challita, W. Saad, and C. Bettstetter, "Interference management for cellular-connected UAVs: A deep reinforcement learning approach," *IEEE Trans. Wireless Commun.*, vol. 18, no. 4, pp. 2125–2140, Apr. 2019.

[39] D. Arthur and S. Vassilvitskii, "k-means++: The advantages of careful seeding," in *Proc. Symp. Discrete Algorithms*, 2017, pp. 1027–1035.

[40] *Performance of eICIC With Control Channel Coverage Limitation*, Standard R1-103264, 3GPP, NTT DOCOMO, Montreal, QC, Canada, 2010.

[41] J. A. del Peral-Rosado, R. Raulefs, J. A. López-Salcedo, and G. Seco-Granados, "Survey of cellular mobile radio localization methods: From 1G to 5G," *IEEE Commun. Surveys Tuts.*, vol. 20, no. 2, pp. 1124–1148, 2nd Quart., 2017.
[42] M. Najla, Z. Becvar, P. Mach, and D. Gesbert, "Predicting device-to-device channels from cellular channel measurements: A learning approach," *IEEE Trans. Wireless Commun.*, vol. 19, no. 11, pp. 7124–7138, Nov. 2020.
[43] Q. Mao, F. Hu, and Q. Hao, "Deep learning for intelligent wireless networks: A comprehensive survey," *IEEE Commun. Surveys Tuts.*, vol. 20, no. 4, pp. 2595–2621, Jun. 2018.
[44] K. I. Ahmed, H. Tabassum, and E. Hossain, "Deep learning for radio resource allocation in multi-cell networks," *IEEE Netw.*, vol. 33, no. 6, pp. 188–195, Nov. 2019.
[45] R. Dong, C. She, W. Hardjawana, Y. Li, and B. Vucetic, "Deep learning for hybrid 5G services in mobile edge computing systems: Learn from a digital twin," *IEEE Trans. Wireless Commun.*, vol. 18, no. 10, pp. 4692–4707, Oct. 2019.
[46] S. Sritharan, H. Weligampola, and H. Gacanin, "A study on deep learning for latency constraint applications in beyond 5G wireless systems," *IEEE Access*, vol. 8, pp. 218037–218061, 2020.
[47] R. I. Bor-Yaliniz, A. El-Keyi, and H. Yanikomeroglu, "Efficient 3-D placement of an aerial base station in next generation cellular networks," in *Proc. IEEE ICC*, May 2016, pp. 1–5.
[48] N. Ahmed, S. S. Kanhere, and S. Jha, "On the importance of link characterization for aerial wireless sensor networks," *IEEE Commun. Mag.*, vol. 54, no. 5, pp. 52–57, May 2016.
[49] A. Al-Hourani, S. Kandeepan, and S. Lardner, "Optimal LAP altitude for maximum coverage," *IEEE Wireless Commun. Lett.*, vol. 3, no. 6, pp. 569–572, Dec. 2014.
[50] M. H. Beale, M. T. Hagan, and H. B. Demuth, *Deep Learning Toolbox: Users Guide*. Boston, MA, USA: Matheworks, 2020.
[51] R. K. Jain, D.-M. W. Chiu, and W. R. Hawe, "A quantitative measure of fairness and discrimination," Eastern Res. Lab., Digit. Equip. Corp., Hudson, MA, USA, Tech. Rep. DEC-TR-301, 1984.

MD. SAKIR HOSSAIN (Member, IEEE) received the B.Sc. and M.Sc. degrees in information and communication engineering from University of Rajshahi, Bangladesh, and the Ph.D. degree in information and computer science from Saitama University, Saitama, Japan. In 2019, he worked as a Postdoctoral Researcher with Czech Technical University in Prague, Prague, Czech Republic. As a postdoctoral researcher, he did research in interference management for unmanned aerial vehicle (UAV) assisted wireless networks. He currently works as an Assistant Professor with the Department of Computer Science, American International University-Bangladesh (AIUB), Bangladesh. Before joining AIUB, he worked with the Department of Electronic and Telecommunications Engineering, International Islamic University Chittagong, Chittagong, Bangladesh. He works on the development of solutions for wireless networks with special focus on UAV assisted wireless networks, intelligent reflecting surface, machine learning assisted wireless networks, waveform design, and cyber-security.

ZDENEK BECVAR (Senior Member, IEEE) received the M.Sc. and Ph.D. degrees in telecommunication engineering from Czech Technical University in Prague, Czech Republic, in 2005 and 2010, respectively. From 2006 to 2007, he joined Sitronics Research and Development Center in Prague focusing on speech quality in VoIP. Furthermore, he was involved in research activities of Vodafone Research and Development Center, Czech Technical University in Prague, in 2009. He was on internships at Budapest Politechnic, Hungary, in 2007; CEA-Leti, France, in 2013; and EURECOM, France, in 2016 and 2019. From 2013 to 2017, he was a representative of the Czech Technical University in Prague in ETSI and 3GPP standardization organizations. In 2015, he founded 5Gmobile research lab, Czech Technical University in Prague, where he is focused on research towards 5G and beyond mobile networks. He is currently an Associate Professor with the Department of Telecommunication Engineering, Czech Technical University in Prague. He has published four book chapters and more than 90 conference or journal articles. He works on the development of solutions for future mobile networks with special focus on optimization of mobility and radio resource management, energy efficiency, device-to-device communication, edge computing, C-RAN, self-optimization, and architecture of radio access networks.